Physics Letters A 383 (2019) 1960–1966

Contents lists available at ScienceDirect

Physics Letters A

www.elsevier.com/locate/pla

Magnetic circular dichroism and absorption spectra of $^5I_8 \rightarrow {}^5F_5$ transition in $HoAl_3(BO_3)_4$ and $HoFe_3(BO_3)_4$ single crystals

A.V. Malakhovskii *, V.V. Sokolov, I.A. Gudim, M.V. Rautskii

Kirensky Institute of Physics, Federal Research Center KSC SB RAS, 660036 Krasnoyarsk, Russian Federation

ARTICLE INFO

Article history:
Received 18 January 2019
Received in revised form 13 March 2019
Accepted 13 March 2019
Available online 20 March 2019
Communicated by V.A. Markel

Keywords:
Ho^{3+} ion
f-f transitions
Magnetic circular dichroism
Electron structure

ABSTRACT

Comparative study of magnetic circular dichroism (MCD) and absorption spectra of $HoAl_3(BO_3)_4$ and $HoFe_3(BO_3)_4$ single crystals in the region of $^5I_8 \rightarrow {}^5F_5$ transition of the Ho^{3+} ion was carried out. Absorption spectra were decomposed into the Lorentz shape components and intensities of transitions were obtained. Unusually strong vibronic transitions were observed in $HoAl_3(BO_3)_4$, but were not observed in $HoFe_3(BO_3)_4$ that testified to the strong non diagonal vibronic interaction in $HoAl_3(BO_3)_4$. The MCD spectra were analyzed in approximation of the $|J, \pm M_J\rangle$ wave functions of the free atom and using concept of the crystal quantum number. Peculiarity of application of this concept to ions with integer moments was revealed and modification of the concept was suggested. With the help of the MCD spectra, the Zeeman splitting of some transitions was found. In particular, the Landé factor $g_C \approx 2$ of the ground state of the Ho^{3+} ion in $HoAl_3(BO_3)_4$ in the trigonal axis direction was determined. It appeared to be five times less than that in $HoFe_3(BO_3)_4$ also found with the help of the MCD.

1. Introduction

$HoAl_3(BO_3)_4$ and $HoFe_3(BO_3)_4$ crystals have huntite-like structure, but different space symmetry. $HoAl_3(BO_3)_4$ crystal possesses $R32$ space symmetry at all temperatures. $HoFe_3(BO_3)_4$ crystal undergoes the structural phase transition from $R32$ to $P3_121$ (D_3^4) symmetry. Temperature of the transition strongly depends on the technology of the crystal growing. So it is 427 K for the powder samples obtained by the solid-state synthesis [1] and 360 K for single crystals grown from a solution-melt [2].

Ho^{3+} activated crystals are widely used in solid state lasers both in the infrared and visible spectral ranges. Optical properties of Ho^{3+} ion were studied in a great variety of materials (e.g. [3–10]). Koporulina et al. [11] investigated visible and near-infrared luminescence in Ho:$YAl_3(BO_3)_4$ crystal. The huntite-like structure has no center of inversion. Therefore, crystals of this structure can be used as nonlinear active media [12,13]. Spectroscopic properties of $HoAl_3(BO_3)_4$ crystal were studied in Ref. [14]. The first study of the optical absorption spectra of $HoFe_3(BO_3)_4$ single crystal in the infrared region (500–10000 cm^{-1}) was presented in Ref. [2]. f-f transitions in $HoFe_3(BO_3)_4$ were studied in detail in the region of 8500–24500 cm^{-1} in the temperature range including the spin-reorientation in Ref. [15] and as a function of magnetic field in Ref. [16].

Investigations of magnetic and magneto-electric properties of the $HoFe_3(BO_3)_4$ single crystal showed that it referred to multiferroics [17,18]. The giant magnetoelectric polarization was also observed in paramagnetic $HoAl_3(BO_3)_4$ in magnetic field [19–21]. Both studied crystals have highly anisotropic magnetic properties at low temperatures [20,22,23]. $HoFe_3(BO_3)_4$ crystal becomes antiferromagnet at temperatures below $T_N = 38$ K [22].

Magnetic circular dichroism (MCD) of f-f transitions in solids is widely studied. We shall mention only investigations related to the Ho^{3+} ion containing compounds [24–26]. MCD consists of the diamagnetic and paramagnetic parts. Temperature dependence of the integral paramagnetic MCD of the parity forbidden f-f absorption bands reveals peculiar behavior and gives information about the nature of the f-f transitions allowance [27]. The present work is devoted to the comparative study of the diamagnetic MCD and absorption spectra of f-f transitions in Ho^{3+} ion in two crystals with the same structure and close symmetry. The diamagnetic MCD permits us to determine the Zeeman splitting of transitions and states. Properties of the excited states are directly connected with the local properties of crystals, which are changed by the optical excitation. This information is important in connection with the modern problem of the quantum information processing. For the interpretation of the results we used presentation of the electron states in the approximation of $|J, \pm M_J\rangle$ wave functions of

* Corresponding author.
E-mail address: malakha@iph.krasn.ru (A.V. Malakhovskii).

https://doi.org/10.1016/j.physleta.2019.03.016
0375-9601/

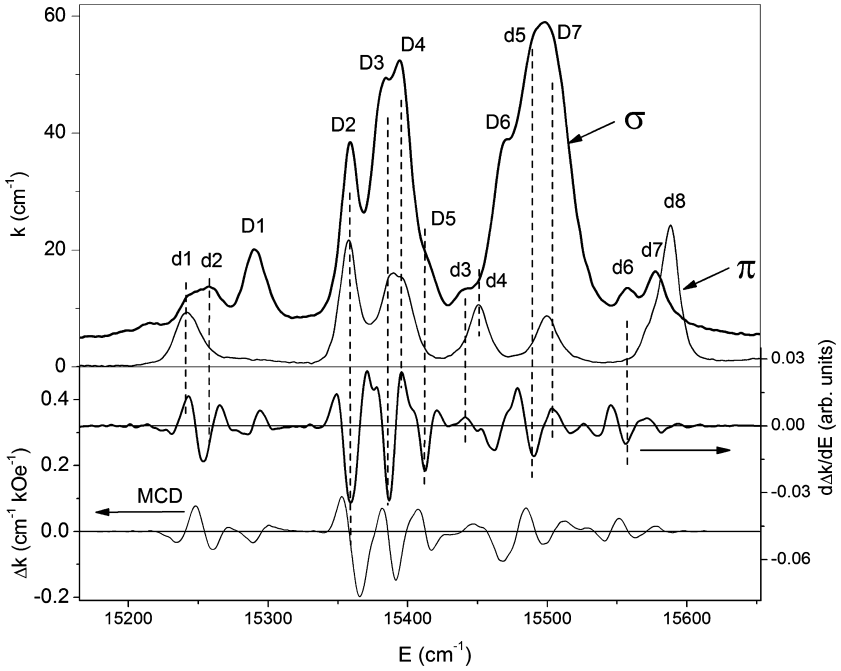

Fig. 1. Polarized absorption and MCD spectra of $HoAl_3(BO_3)_4$ single crystal at 90 K.

the free atom and the concept of the crystal quantum number suggested by Elyashevich [28]. A peculiarity of application of this concept to ions with integer moments was revealed and discussed.

2. Experimental details

$HoAl_3(BO_3)_4$ crystals were grown from the melt solution based on bismuth trimolybdate and lithium molybdates using the technique described in [29]. $HoFe_3(BO_3)_4$ single crystals were grown from a bismuth trimolibdate solution-melt with a nonstoichiometric composition of the crystal forming oxides. The technology was described in detail in Ref. [15].

As mentioned above, the crystals have huntite-like structure and the trigonal symmetry. The lattice constants of the $HoAl_3(BO_3)_4$ are: $a = 9.293(3)$ Å, $c = 7.240(3)$ Å [30] and those of $HoFe_3(BO_3)_4$ are $a = 9.53067(5)$ Å, $c = 7.55527(6)$ Å [22]. The unit cell contains three formula units. Trivalent RE ions are located at the center of trigonal prisms of the D_3 symmetry in $HoAl_3(BO_3)_4$ and of the C_2 symmetry in $HoFe_3(BO_3)_4$. The prisms are made up of six oxygen ions. The FeO_6 and AlO_6 octahedrons share edges in such a way that they form helicoidal chains, which run parallel to the trigonal C_3 axis of the crystal and are mutually independent.

The absorption spectra were measured by the two beam technique, using an automated spectrophotometer designed on the basis of the diffraction monochromator MDR-2. Optical slit width (spectral resolution) was 0.2 nm in the region of 300–600 nm and 0.4 nm in the region of 600–1100 nm. The spectra were obtained in α-polarization, i.e., the light propagated along the trigonal C_3 axis, and also when light propagated perpendicular to the C_3 axis: for electric vector of the light wave perpendicular to the C_3 axis (σ-polarization) and parallel to the C_3 axis (π-polarization). The α- and σ-polarized spectra coincided within the limit of the experimental error that testified to the electric dipole character of the absorption.

The MCD spectra were recorded with the light propagating along the C_3 axis of the crystals. The magnetic field of 5 kOe was also directed along the C_3 axis. The circular dichroism was measured using the modulation of the light wave polarization with the piezoelectric modulator (details see in Ref. [31]). The MCD was obtained as a half difference of the circular dichroisms at opposite magnetic fields. The natural circular dichroism is excluded in this case. The sensitivity in measuring of the circular dichroism was 10^{-4}, and the spectral resolution was the same as that at the absorption spectra measuring. The sample was put in a nitrogen gas flow cryostat. Accuracy of the temperature measuring was ~ 1 K. Thickness of the $HoAl_3(BO_3)_4$ samples was 0.25 mm and that of the $HoFe_3(BO_3)_4$ samples was 0.19 mm.

The EPR measurements were performed on the equipment of the KRCCU FRC KSC SB RAS (spectrometer ELEXSYS E580, Bruker, Germany) at the frequency 9.07 GHz.

3. Results

Polarized absorption and MCD spectra of the $^5I_8 \rightarrow {}^5F_5$ absorption band are presented in Figs. 1 and 2. The absorption spectra were decomposed into the Lorentz shape components and their intensities were determined (see Table 1). The capital letters in Figs. 1, 2 and in Table 1 indicate transitions from the ground state and the lower case characters indicate transitions from the upper states of the ground multiplet or vibronic transitions. Symmetries of states or identification of transitions from the upper states of the ground multiplet are shown in Table 1 in brackets.

The MCD of a doublet in magnetic field directed along the light propagation is given by the equation:

$$\Delta k = k_{m+}\varphi(\omega, \omega_0 + \Delta\omega_0) - k_{m-}\varphi(\omega, \omega_0 - \Delta\omega_0). \quad (1)$$

Here k_{m+} and k_{m-} are amplitudes of (+) and (−) circularly polarized lines; φ are form functions of (+) and (−) polarized lines. If the Zeeman splitting $\Delta\omega_0$ is much less than the line width then:

$$\Delta k = k_m c\varphi(\omega, \omega_0) + k_m \Delta\omega_0 \partial\varphi(\omega, \omega_0)/\partial\omega_0. \quad (2)$$

Here $k_m = k_{m+} + k_{m-}$ is the amplitude of the line not split by the magnetic field and $c = (k_{m+} - k_{m-})/k_m$. The first term in (2) is the paramagnetic MCD and the second one is the diamagnetic effect. Thin structure of the MCD spectra (Figs. 1, 2) is due to the diamagnetic effect. Integral of the MCD spectrum over multiplet gives the integral paramagnetic MCD of the multiplet (integral of the diamagnetic part is zero).

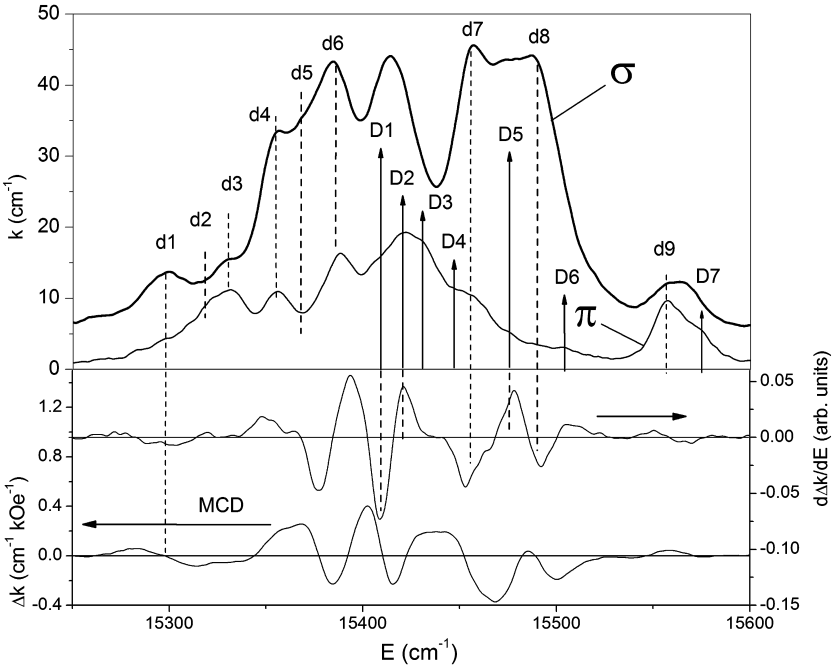

Fig. 2. Polarized absorption and MCD spectra of $HoFe_3(BO_3)_4$ single crystal at 90 K.

Table 1
Energies of states or transitions (E) and intensities of transitions (I) at 90 K. Symmetries of states or types of transitions are shown in brackets. Δg_C is the experimental change of the Landé factor along the C_3 axis during transition.

Multiplets	Levels, transitions	$HoAl_3(BO_3)_4$				$HoFe_3(BO_3)_4$			
		E (cm^{-1})	Intensity I_π (cm^{-2})	Intensity I_σ (cm^{-2})	Δg_C	E (cm^{-1})	Intensity I_π (cm^{-2})	Intensity I_σ (cm^{-2})	Δg_C
$^5I_8$ (Gr)	Gr1	0 (E_1)				0 (E)			
	Gr2	16 (E)				9 (A)			
	Gr3	17 (A_1)				12 (E)			
	Gr4	33 (A_2)				16 (A)			
	Gr5	99 (A)				21 (E)			
	Gr6	118 (E)				47 (A)			
	Gr7					58 (A_2)			
	Gr8					67 (A?)			
$^5F_5$ (D)						D1a 15405	214	0	
	D1	15291 (A_1)	0	329	(−)	15412 (A_1)	0	677	−10.2
	D2	15359 (E_2)	422	538	−1.5	15420 (E)	533	534	(+)
	D3	15382 (E_1)	326	727	(−)	15430 (E)	250	σ	
	D4	15396 (E_2)	177	1014	(+)	15446 (E)	π	σ	
	D5	15413 (A_2)	0	40	(−)	15474 (A_2)	0	1320	(+)
	D6	15467 (A_2)	0	326	(−)?	15500 (A_2)	0	237	
	D7	15503 (E_1)	218	1616	(−)?	15574 (E)	97	102	
	d1	15241.3 (Gr6-D2)	291	164	+3.5	15299	126	407	−14.6
	d2	15260 (Gr5-D2)	0	114	(−)?	15322	240	0	
	d3	15439.5 (?)	0	50(?)	(+)	15329	97	42	
	d4	15450.5 (Gr3-D6)	228	0	0	15354	200	575	
	d5	15489 (?)	0	1376	(−)	15367	0	228	
	d6	15557.1 (D6+87,1)	0	39	−2.1	15385	306	1305	
	d7	15578.3 (D6+108.3)	127	211	−0.6	15454	352	733	(−)
	d8	15588 (Gr3-D7+102)	450	0	0	15489 (Gr3-D6)	0	500	(−)
	d9					15556 (Gr5-D7)	211	142	

Diamagnetic MCD of the distinct lines is not always spectrally resolved. However, it is possible to define signs of the diamagnetic MCD ($\Delta\omega_0$) with the help of the first derivative of the MCD. For the MCD written in the form (1), it is possible to show [27] that signs of extrema of the function $\partial\Delta k/\partial\omega$ at positions of the absorption lines give signs of the diamagnetic effect ($\Delta\omega_0$). Thus we find signs of the diamagnetic effects of the transitions from the experimental MCD spectra (Figs. 1, 2, Table 1). The purely π-polarized lines, evidently, have no MCD.

If the MCD spectra of transitions are well resolved, it is possible to find values of the Zeeman splitting $\Delta\omega_0$ from the absorption and MCD spectra. According to Ref. [27] for the Lorentz shape of the absorption line (as in our case) it is:

$$\Delta\omega_0 = 2\frac{\Delta k_{dm}}{k_m}|\omega_m - \omega_0|. \tag{3}$$

Here Δk_{dm} and ω_m are the value and position of extrema of the diamagnetic MCD of the line, respectively, and k_m is amplitude

Table 2
Selection rules for electric dipole transitions in the D_3 symmetry.

	A_1	A_2	E
A_1	–	π	$\sigma(\alpha)$
A_2	π	–	$\sigma(\alpha)$
E	$\sigma(\alpha)$	$\sigma(\alpha)$	$\pi, \sigma(\alpha)$

of the α-absorption of the line. The experimental changing of the Landé factor Δg_C during transitions (Table 1) were found from the Zeeman splitting of the transitions in magnetic field directed along the C_3 axis of the crystals:

$$2\hbar\Delta\omega_0 = \mu_B H \Delta g_C. \tag{4}$$

4. Discussion

4.1. $HoAl_3(BO_3)_4$

Ho^{3+} ions are located in the D_3 symmetry positions in $HoAl_3(BO_3)_4$ crystal. At the conversion from a free atom to that in octahedron and further to the D_3 symmetry position, the ground and discussed excited state of the Ho^{3+} ion are transformed in the following way:

$$^5I_8(J=8) \to A_1 + 2E + 2T_1 + 2T_2 \to A_1 + 2E + 2(A_2 + E) + 2(A_1 + E). \tag{5}$$

$$^5F_5(J=5) \to E + 2T_1 + T_2 \to E + 2(A_2 + E) + (A_1 + E). \tag{6}$$

If the ground state was of the A_1 type, then according to the selection rules (Table 2) we would have $\sigma + 2(\pi + \sigma) + (0 + \sigma)$ lines. If the ground state was of the A_2 type, then there would be $\sigma + 2(0 + \sigma) + (\pi + \sigma)$ lines. If the ground state was of the E type, then there would be $\pi\sigma + 2(\sigma + \pi\sigma) + (\sigma + \pi\sigma)$ lines. The latter situation is the very thing which is observed (Fig. 1, Table 1). The same polarization of lines was observed in $HoFe_3(BO_3)_4$ at $T = 2$ K [15]. Consequently, the local symmetry of the Ho^{3+} ion in $HoFe_3(BO_3)_4$ is also close to the D_3 one and in both cases polarizations of the absorption lines correspond to the transitions from the ground state of the E-symmetry. According to [32], in $HoAl_3(BO_3)_4$ there is a singlet state 1.2 cm^{-1} below the considered E-state, that is, there are two practically coincided states. However, the above consideration shows, that transitions from singlet states give polarizations, which are not observed. According to the Yahn–Teller theorem, the ground state of ion with the integer moment should be a singlet. Apparently, the electron-vibrational interaction is very small and a splitting of the E-state is not observed. Additionally, Baraldi et al. [6] found that the lowest level in YAB:Ho crystal is also the E-doublet.

Unusually strong vibronic lines d6, d7 and d8 were revealed in the $HoAl_3(BO_3)_4$ crystal (Fig. 1). Vibrations of the A_2 and E symmetry (81 and 105 cm^{-1}, respectively) with participation of the rare earth (RE) ion were found in the $YbAl_3(BO_3)_4$ in Ref. [33]. Energy of vibrations weakly depends on type of the RE ion, and we can use these values for holmium alumoborate in a first approximation. Mentioned vibrations create the following vibronic states with the excited electronic state D6 of the A_2 symmetry: $A_2 \times A_2 = A_1$, $A_2 \times E = E$. Taking into account polarizations of the d6 and d7 vibronic lines (Fig. 1, Table 1) and the selection rules of Table 2, we obtain from the absorption spectrum (Fig. 1) the local vibrations 87 cm^{-1} (A_2) and 108 cm^{-1} (E) in the excited state D6 (A_2) (Table 1). The line d8 is also due to a vibronic transition, however its π-polarization shows that, according to the selection rules (Table 2), the transition occurs from one of the upper sublevels of the ground multiplet with the A-symmetry and the final state also should have A-symmetry. It is easy to check that the energy of the transition from the lowest level Gr3 of the ground multiplet with the A-symmetry into the vibronic $D6(A_2) + A_2$ state is substantially less than the d8 transition energy. The only possible scheme of the d8 transition from the point of view of its energy is: $Gr3(A_1) \to D7(E) + E$ with the energy of the E-vibration of 102 cm^{-1}. However, the electron state D7 of the E-symmetry creates with the E-vibration the vibronic states: $E \times E = A_1 + A_2 + E$, and we have to suppose that transition into the vibronic E-state is not observed, but transition $Gr3(A_1) \to A_2$ is observed. Obtained energy 102 cm^{-1} well corresponds to that found in [33].

Selection rules of Table 2 make it possible to analyze linear polarizations of transitions, but not circular polarizations in magnetic field. Such possibility is given by the concept of the crystal quantum number suggested in [28] for electron states in crystals of the axial symmetry. For the states with the integer momentum the crystal quantum number μ has values: $\mu = 0, +1, -1$ in trigonal crystals. Additionally, the electron states in the uniaxial crystals can be described in a first approximation by the $|J, \pm M_J\rangle$ wave functions of the free atom. Between values of μ, M_J and irreducible representations of states there is the following correspondence [28]:

$$M_J = 0 \quad \pm 1 \quad \pm 2 \quad (\pm 3)_{1,2} \quad \pm 4 \quad \pm 5 \quad (\pm 6)_{1,2} \quad \pm 7 \quad \pm 8 \tag{7}$$

$$\mu = 0 \quad \pm 1 \quad \mp 1 \quad 0 \quad \pm 1 \quad \mp 1 \quad 0 \quad \pm 1 \quad \mp 1 \tag{8}$$

$$A_1 \quad E_1 \quad E_2 \quad A_1, A_2 \quad E_1 \quad E_2 \quad A_1 A_2 \quad E_1 \quad E_2 \tag{9}$$

The doublets E_1 and E_2 differ by signs of μ.

The projection M_J defines the splitting of the state in magnetic field. Correspondingly, the Landé factor g_{CM} of the $\pm M_J$ doublet in the $|J, \pm M_J\rangle$ wave functions approximation is:

$$g_{CM} = 2gM_J, \tag{10}$$

where g is the Landé factor of the free atom (see Table 3). Then we can theoretically estimate the changes of the Landé factor Δg_{CM} for transitions between states. It was earlier made in crystals with the half integer moments of the rare earth ions (e.g. [27,34]). Rather good correspondence between the theory and experiment was obtained for a number of transitions but not for all of them. Sometimes even signs of results were different.

Application of the crystal quantum number concept to ions with the integer moment (such as Ho^{3+}) revealed some features in comparison with ions with the half integer moments. In order to understand these features, it is necessary to draw typical diagrams of states and transitions in both types of ions (see Figs. 3a, 3b). A fragment of the real diagram of states and transitions in $ErAl_3(BO_3)_4$ is presented in Fig. 3a [34]. For ions with the half integer moments the correspondence between M_J, μ and irreducible representations of states has the form:

$$M_J = \pm 1/2, \pm 3/2, \pm 5/2, \pm 7/2, \pm 9/2, \pm 11/2, \pm 13/2, \pm 15/2$$

$$\mu = \pm 1/2, (\pm 3/2), \mp 1/2, \pm 1/2, (\pm 3/2), \mp 1/2, \pm 1/2, (\pm 3/2)$$

$$E_{1/2} \quad E_{3/2} \quad E_{1/2} \quad E_{1/2} \quad E_{3/2} \quad E_{1/2} \quad E_{1/2} \quad E_{3/2} \tag{11}$$

In [28] the selection rules for the number μ in crystals were presented, which were similar to those for the number M_J in free atoms. In particular, for the electric dipole absorption

$$\Delta\mu = \pm 1 \text{ corresponds to } \mp \text{ circularly polarized and } \sigma\text{-polarized waves}, \tag{12}$$

$$\Delta\mu = 0 \text{ corresponds to } \pi\text{-polarized waves.}$$

Table 3
Landé factors of states g_{CM} along the C_3 axis in the $|J, \pm M_J\rangle$ function approximation. g is the Landé factor of a free ion.

State	M_J / g	8	7	6	5	4	3	2	1	0
$^5I_8$ (Gr)	1.25	20	17.5	15	12.5	10	7.5	5	2.5	0
$^5F_5$ (D)	1.40				14	11.2	8.4	5.6	2.8	0
		E_2	E_1	A_1A_2	E_2	E_1	A_1A_2	E_2	E_1	A_1

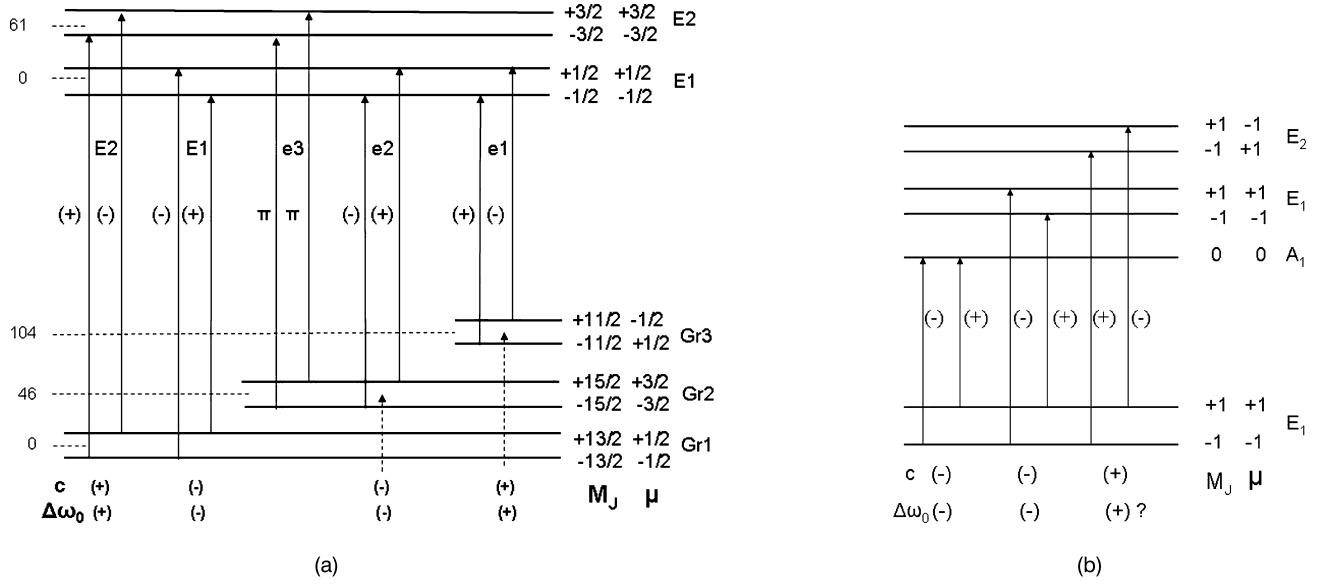

Fig. 3. (a) Diagram of the electron states and transitions in $ErAl_3(BO_3)_4$ crystal [34]. (b) Diagram of the main types of electron states and transitions in $HoAl_3(BO_3)_4$ crystal.

For the linearly polarized waves, these selection rules coincide with those of Table 2. The selection rules (12) permitted us to create the diagram of MCD of all types of transitions (see Fig. 3a) and to predict not only value but also sign of the Zeeman splitting of some transitions [34].

Substantially different situation is observed in ions with the integer moments (see typical diagram in Fig. 3b). Circularly polarized (and, correspondingly, σ-polarized) E-E transitions are forbidden according to selection rules (12) that contradicts to the experiment and to the symmetry selection rules of Table 2. Thus, we have to infer, that the selection rules (12) are not strict. Selection rules of the type (12) are strict only for M_J. For example, transition $M_J = \pm 1 \rightarrow M_J = \pm 4$ is forbidden. However in crystals the states with different M_J but equal μ are mixed. In particular, if the state $M_J = \pm 2$ is admixed to the state $M_J = \pm 4$, then the considered transition will be partially allowed. Thus, the splitting of states and transitions in magnetic field is defined by the main part of the wave function of the $|J, \pm M_J\rangle$ type with $M_J = M_{eff}$, while the polarization and the intensity of the transition are defined by the admixtures caused by the crystal field. The even part of the crystal field mixes states with the different M_J, and the odd part of the crystal field mixes states with the different parity and so partially allows f-f transitions. As a result it is possible to explain cases, when the experimental value of the Zeeman splitting coincides with the theoretical prediction but the sign is opposite.

Basing on the necessity of the coincidence of the selection rules for electron transitions between states characterized by the crystal quantum number μ and by the irreducible representations, we can suggest instead (12) another selection rules for μ, which are suitable both for states with integer and half integer moments:

$$\Delta\mu = \pm 1, \pm 2 \text{ corresponds to } \mp \text{ circularly polarized and } \sigma\text{-polarized waves,} \quad (13)$$

Table 4
Signs of the Zeeman splitting of transitions.

	A	E_1	E_2
$A \rightarrow$	0	(+)	(−)
$E_1 \rightarrow$	(−)	(−)	(+, −)
$E_2 \rightarrow$	(+)	(−, +)	(+)

$\Delta\mu = 0$ corresponds to π-polarized waves or are forbidden (see Table 2).

Diagram of Fig. 3b was created basing on the selection rules (13). From the above consideration it is clear that the selection rules (12) and (13) are not strict and are useful only for the preliminary estimation of the situation. It is seen from Fig. 3b that sign of the Zeeman splitting of the $E_1 \rightarrow E_2$ transition depends on the correlation between values of the Zeeman splitting of the ground and excited states. Basing on the diagrams similar to that shown in Fig. 3b, it is possible to create Table 4 of signs of the Zeeman splitting for all types of the transitions. First signs for transitions $E_1 \leftrightarrow E_2$ refer to the cases, when splitting of the initial state is larger than that of the final state.

It is evident, that the Zeeman splitting of the transition $E \rightarrow A$ from the ground state will give the Zeeman splitting and the Landé factor of the ground state. One of such transitions (d6 in Fig. 1) permitted us to find $g_C = -2.1$ (the sign corresponds to sign of the Zeeman splitting). In Ref. [20] from magnetic measurements and crystal field calculations it was obtained that $g_C = 2.52$. From the EPR spectrum (Fig. 4) measured at the room temperature in the field $H \parallel C_3$ we found the Landé factor $g_C = 2$ (± 0.05). The latter value we accepted for the subsequent analysis. The listed values of g_C are close to the theoretical $g_{CM} = 2.5$ for the state $M_J = 1$ (see Table 3). The difference between the theoretical and experimental

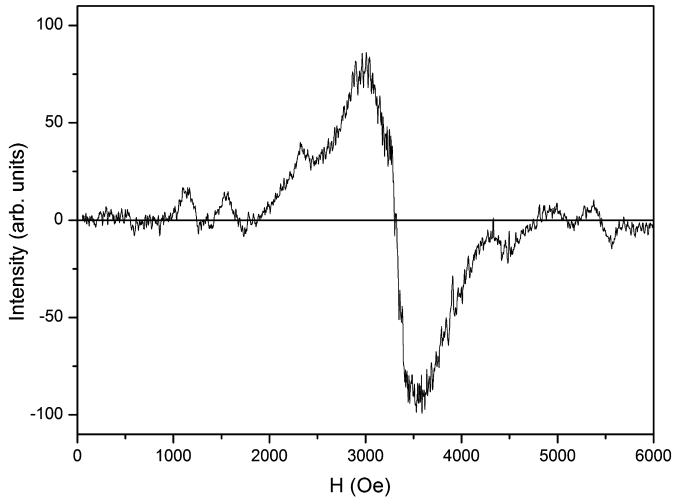

Fig. 4. EPR spectrum of $HoAl_3(BO_3)_4$ crystal in the field $H \parallel C_3$ at the room temperature.

values is due to the mentioned above mixing of states with the different M_J by the crystal field. $M_J = 1$ corresponds to the state of the E_1 type (see Eqs. (7)–(9)), and, according to Fig. 3b, the transition $E_1 \rightarrow A$ should have negative Zeeman splitting that is really observed.

Taking into account that $g_C = 2$ in the ground state of the E_1 type, $\Delta g_C = -1.5$ of transition $\mathrm{Gr1}(E_1) \rightarrow \mathrm{D2}$ (see Table 1) means, that 1) the D2 doublet is of the E_2 type according to diagram of Fig. 3b, 2) the splitting of the D2 excited state is larger than that of the ground state and 3) the D2 state Landé factor is: $g_C = 3.5$. Table 3 testifies that, most probably, D2 is the state with the theoretical $M_J = 2$ modified by the crystal field. According to Eq. (12), but being applied to M_J, transitions from the ground state $M_J = 1$ are allowed only in the states $M_J = 0$ and $M_J = 2$. All the rest transitions are allowed only due to the mixing of the states.

4.2. $HoFe_3(BO_3)_4$

For the identification of states and as initial information for the decomposition of the absorption spectrum into the Lorentz shape components at 90 K we used absorption spectra of $HoFe_3(BO_3)_4$ at 5.8 K [15]. Positions of the absorption lines at 5.8 K are shown by arrows in Fig. 2. The temperature 5.8 K is already above the reorientation transition, and positions of the absorption lines weakly change with the subsequent increasing of the temperature. Number of the absorption lines and their polarizations in $HoFe_3(BO_3)_4$ correspond in a first approximation to the local symmetry D_3 and succession of the lines [15] coincides with that in $HoAl_3(BO_3)_4$. Only the D1 line presents the exclusion: it splits and acquires π-polarization above the reorientation transition (see [15,16]). Thus, we can consider the $HoFe_3(BO_3)_4$ spectrum mainly in the D_3 symmetry approximation, and, in particular, the ground state has E-symmetry in this approximation [15]. From the MCD spectrum (Fig. 2) and with the help of decomposition of the σ-spectrum into the Lorentz components we found the Zeeman splitting of the transition D1 ($E \rightarrow A$) (see Eq. (3)) and, consequently, the Landé factor of the ground state: $g = -10.2$ that corresponded to $M_{Jeff} \approx 4$ (see Table 3) in contrast to $M_{Jeff} = 0.8$ in $HoAl_3(BO_3)_4$. Negative sign of the Landé factor means that the ground state is of the E_1 type that corresponds to diagram of Fig. 3b. Earlier, basing on the magnetic measurements, in Ref. [15] it was also shown that the ground E-state in $HoFe_3(BO_3)_4$ had $M_{Jeff} = 4$. Strong difference of the Landé factor of the Ho^{3+} ground state in $HoFe_3(BO_3)_4$ and $HoAl_3(BO_3)_4$ crystals shows, that parameters of the crystal field in these crystals are substantially different in spite of the close local symmetry. The d1 line (Fig. 2) with $\Delta g_C = -14.6$ (Table 1) most probably corresponds to the transition $|J = 8, M_J = 8\rangle \rightarrow |J = 5, M_J = 1\rangle$ from one of the upper components of the ground multiplet with the theoretical $\Delta g_{CM} = -17.2$ (see Tables 3 and 4).

The total crystal field splitting of the considered absorption band is 212 cm^{-1} in $HoAl_3(BO_3)_4$, while it is 168 cm^{-1} in $HoFe_3(BO_3)_4$ (see Table 1) and their ratio is 1.26. This indicates that even part of the crystal field in the $^5F_5$ state is larger in $HoAl_3(BO_3)_4$ as compared with that in $HoFe_3(BO_3)_4$. The sum intensity $(2I_\sigma + I_\pi)$ of the Σ(D1-D6) transitions from the ground state in $HoAl_3(BO_3)_4$ is 1.51 times larger than that in $HoFe_3(BO_3)_4$. This means that odd part of the crystal field, which allows f-f transitions, is also larger in $HoAl_3(BO_3)_4$. Both features correspond to smaller lattice constants of the $HoAl_3(BO_3)_4$ (see Section 2 of the present paper). Intensities of transitions from the upper components of the ground multiplet are larger in $HoFe_3(BO_3)_4$ than in $HoAl_3(BO_3)_4$ (Figs. 1 and 2).

The vibrational satellites of the electron transitions, both from the lowest and upper sublevels of the ground multiplet, similar to d6, d7 and d8 lines in $HoAl_3(BO_3)_4$ (Fig. 1), are not observed in $HoFe_3(BO_3)_4$ (Fig. 2). This testifies to the weak non diagonal vibronic interaction in $HoFe_3(BO_3)_4$.

Peculiar behavior of the D1 transition in $HoFe_3(BO_3)_4$ was already mentioned: it appeared in π-polarization at temperature above the reorientation transition. This was explained in Ref. [16] by decrease of the local symmetry during the D1 transition both in the initial and final states. Such decrease of the local symmetry not only in the final but also in the initial state during the electron transition is possible, because according to the perturbation theory electron transitions occur due to mixing of the initial and final states by perturbation caused by the electromagnetic wave. Therefore, during the electron transition, the initial state of the ion and its interaction with the environment can also change.

5. Summary

Comparative study of the MCD and absorption spectra of $HoAl_3(BO_3)_4$ and $HoFe_3(BO_3)_4$ single crystals in the region of $^5I_8 \rightarrow {}^5F_5$ transition of the Ho^{3+} ion was carried out. Absorption spectra were decomposed into the Lorentz shape components and intensities of transitions were obtained. Strong vibronic transitions were observed in $HoAl_3(BO_3)_4$, but not observed in $HoFe_3(BO_3)_4$ that testified to the strong non diagonal vibronic interaction in $HoAl_3(BO_3)_4$. It was shown that even and especially odd part of the crystal field in the $^5F_5$ state are larger in $HoAl_3(BO_3)_4$ than those in $HoFe_3(BO_3)_4$, that corresponds to smaller lattice constants of the $HoAl_3(BO_3)_4$ crystal. Local symmetry of the Ho^{3+} ion in $HoFe_3(BO_3)_4$ is C_2, however number and linear polarization of the absorption lines correspond to the D_3 symmetry. MCD spectra were analyzed in approximation of the $|J, \pm M_J\rangle$ wave functions of the free atom and using concept of the crystal quantum number. Peculiarity of application of this concept to ions with integer moments was revealed and modification of the conception was suggested. In particular, the selection rules for the circularly polarized light, consistent with the experiment and with the selection rules for the linear polarizations, were suggested. With the help of the MCD spectra, the Zeeman splitting of some transitions was found. In particular, the Landé factor $g_C \approx 2$ of the ground state of the Ho^{3+} ion in $HoAl_3(BO_3)_4$ in the trigonal axis direction was determined. It appeared to be five times less than that in $HoFe_3(BO_3)_4$ also found with the help of the MCD.

Acknowledgement

The work was supported by the Russian Foundation for Basic Researches grant 19-02-00034.

References

[1] Y. Hinatsu, Y. Doi, K. Ito, M. Wakeshima, A. Alemi, Magnetic and calorimetric studies on rare-earth iron borates $LnFe_3(BO_3)_4$ (Ln= Y, La–Nd, Sm–Ho), J. Solid State Chem. 172 (2003) 438–445.

[2] D.A. Erofeev, E.P. Chukalina, L.N. Bezmaternykh, I.A. Gudim, M.N. Popova, High-resolution spectroscopy of $HoFe_3(BO_3)_4$ crystal: a study of phase transitions, Opt. Spectrosc. 120 (2016) 558–565.

[3] C.S. Rao, K.U. Kumar, P. Babu, C.K. Jayasankar, Optical properties of Ho^{3+} ions in lead phosphate glasses, Opt. Mater. 35 (2012) 102–107.

[4] I. Földvári, A. Baraldi, R. Capelletti, N. Magnani, L.A. Kappers, A. Watterich, Optical absorption and luminescence of Ho^{3+} ions in Bi_2TeO_5 single crystal, Opt. Mater. 29 (2007) 688–696.

[5] Y. Yang, B. Yao, B. Chen, C. Wang, G. Ren, X. Wang, Judd–Ofelt analysis of spectroscopic properties of Tm^{3+}, Ho^{3+} doped $GdVO_4$ crystals, Opt. Mater. 29 (2007) 1159–1165.

[6] A. Baraldi, R. Capelletti, M. Mazzera, N. Magnani, I. Földvári, E. Beregi, Hyperfine interactions in YAB:Ho^{3+}: a high-resolution spectroscopy investigation, Phys. Rev. B 76 (2007) 165130.

[7] L.F. Johnson, H.J. Guggenheim, Infrared pumped visible laser, Appl. Phys. Lett. 19 (1971) 44–47.

[8] B. Zhou, E.Y.B. Pun, H. Lin, D. Yang, L. Huang, Judd–Ofelt analysis, frequency upconversion, and infrared photoluminescence of Ho^{3+}-doped and Ho^{3+}/Yb^{3+}-codoped lead bismuth gallate oxide glasses, J. Appl. Phys. 106 (2009) 103105.

[9] G. Dominiak-Dzik, S. Golab, J. Zawadzka, W. Ryba-Romanowski, T. Lukasiewicz, M. Swirkowicz, Spectroscopic properties of holmium doped crystals, J. Phys. Condens. Matter 10 (1998) 10291.

[10] Li Feng, Jing Wang, Qiang Tang, Lifang Liang, Hongbin Liang, Su Qiang, Optical properties of Ho^{3+}-doped novel oxyfluoride glasses, J. Lumin. 124 (2007) 187–194.

[11] E.V. Koporulina, N.I. Leonyuk, D. Hansen, K.L. Bray, Flux growth and luminescence of Ho: $YAl_3(BO_3)_4$ and $PrAl_3(BO_3)_4$ crystals, J. Cryst. Growth 191 (1998) 767–773.

[12] P. Dekker, J.M. Dawes, J.A. Piper, Y.G. Liu, J.Y. Wang, 1.1 W CW self-frequency-doubled diode-pumped Yb: $YAl_3(BO_3)_4$ laser, Opt. Commun. 195 (2001) 431–436.

[13] E. Cavalli, A. Speghini, M. Bettinelli, M.O. Ramirez, J.J. Romero, L.E. Bausa, J.G. Sole, Luminescence of trivalent rare earth ions in the yttrium aluminium borate non-linear laser crystal, J. Lumin. 102 (2003) 216–219.

[14] D.A. Ikonnikov, A.V. Malakhovskii, A.L. Sukhachev, V.L. Temerov, A.S. Krylov, A.F. Bovina, A.S. Aleksandrovsky, Spectroscopic properties of $HoAl_3(BO_3)_4$ single crystal, Opt. Mater. 37 (2014) 257–261.

[15] A.V. Malakhovskii, S.L. Gnatchenko, I.S. Kachur, V.G. Piryatinskaya, I.A. Gudim, Low-temperature absorption spectra and electron structure of $HoFe_3(BO_3)_4$ single crystal, Low Temp. Phys. 43 (2017) 610–616.

[16] A.V. Malakhovskii, S.L. Gnatchenko, I.S. Kachur, V.G. Piryatinskaya, I.A. Gudim, Transformation of the $HoFe_3(BO_3)_4$ absorption spectra at reorientation magnetic transitions and local properties in the excited $^5F_5$ states of the Ho^{3+} ion, Phys. Rev. B 96 (2017) 224430.

[17] R.P. Chaudhury, F. Yen, B. Lorenz, Y.Y. Sun, L.N. Bezmaternykh, V.L. Temerov, C.W. Chu, Magnetoelectric effect and spontaneous polarization in $HoFe_3(BO_3)_4$ and $Ho_{0.5}Nd_{0.5}Fe_3(BO_3)_4$, Phys. Rev. B 80 (2009) 104424.

[18] A.M. Kadomtseva, Y.F. Popov, G.P. Vorob'ev, A.P. Pyatakov, S.S. Krotov, K.I. Kamilov, L.N. Bezmaternykh, Magnetoelectric and magnetoelastic properties of rare-earth ferroborates, Low Temp. Phys. 36 (2010) 511–521.

[19] K.-C. Liang, R.P. Chaudhury, B. Lorenz, Y.Y. Sun, L.N. Bezmaternykh, V.L. Temerov, C.W. Chu, Giant magnetoelectric effect in $HoAl_3(BO_3)_4$, Phys. Rev. B 83 (2011) 180417.

[20] A.I. Begunov, A.A. Demidov, I.A. Gudim, E.V. Eremin, Features of the magnetic and magnetoelectric properties of $HoAl_3(BO_3)_4$, JETP Lett. 97 (2013) 528–534.

[21] A.L. Freydman, A.D. Balaev, A.A. Dubrovskiy, E.V. Eremin, V.L. Temerov, I.A. Gudim, Direct and inverse magnetoelectric effects in $HoAl_3(BO_3)_4$ single crystal, J. Appl. Phys. 115 (2014) 174103.

[22] C. Ritter, A. Vorotynov, A. Pankrats, G. Petrakovskii, V. Temerov, I. Gudim, R. Szymczak, Magnetic structure in iron borates $RFe_3(BO_3)_4$ (R= Y, Ho): a neutron diffraction and magnetization study, J. Phys. Condens. Matter 20 (2008) 365209.

[23] A.A. Demidov, D.V. Volkov, Magnetic properties of $HoFe_3(BO_3)_4$, Phys. Solid State 53 (2011) 985–996.

[24] D.M. Moran, F.S. Richardson, Measurement and analysis of circular dichroism in the 4f-4f transitions of Ho^{3+} in Na3 [Ho (C4H4O5) 3]. 2NaClO4. $6H_2O$, Inorg. Chem. 31 (1992) 813–818.

[25] M.A. Laguna-Marco, J. Chaboy, H. Maruyama, Element-selective thermal x-ray magnetic circular dichroism study through the magnetic compensation temperature of Ho_6Fe_{23}, Phys. Rev. B 72 (2005) 094408.

[26] K. Fukui, H. Ogasawara, A. Kotani, I. Harada, H. Maruyama, N. Kawamura, K. Kobayashi, J. Chaboy, A. Marcelli, X-ray magnetic circular dichroism at rare-earth $L_{2,3}$ edges in R_2Fe_{14} B compounds (R= La, Pr, Nd, Sm, Gd, Tb, Dy, Ho, Er, Tm, Yb, and Lu), Phys. Rev. B 64 (2001) 104405.

[27] A.V. Malakhovskii, A.L. Sukhachev, A.Yu. Strokova, I.A. Gudim, Magneto-optical activity of $f-f$ transitions and properties of 4f states in single-crystal $DyFe_3(BO_3)_4$, Phys. Rev. B 88 (2013) 075103.

[28] M.A. El'yashevitch, Spectra of Rear Earths, GIT-TL, Moscow, 1953 (in Russian).

[29] V.L. Temerov, A.E. Sokolov, A.L. Sukhachev, A.F. Bovina, I.S. Edelman, A.V. Malakhovskii, Optical properties of trigonal single crystals (Yb, Tm)Al_3 $(BO_3)_4$ grown from fluxes based on the bismuth and lithium molybdates, Crystallogr. Rep. 53 (2008) 1157–1162.

[30] N.I. Leonyuk, L.I. Leonyuk, Growth and characterization of $RM_3(BO_3)_4$ crystals, Prog. Cryst. Growth Charact. Mater. 31 (1995) 179–278.

[31] A.V. Malakhovskii, S.L. Gnatchenko, I.S. Kachur, V.G. Piryatinskaya, A.L. Sukhachev, I.A. Gudim, Optical and magneto-optical properties of $Nd_{0.5}Gd_{0.5}Fe_3(BO_3)_4$ single crystal in the near IR spectral region, J. Alloys Compd. 542 (2012) 157–163.

[32] D. Neogy, K.N. Chattopadhyay, P.K. Ccakrabarti, H. Sen, B.M. Wanklyn, Magnetic behavior of Ho^{3+} in $HoAl_3(BO_3)_4$, J. Magn. Magn. Mater. 154 (1996) 127–132.

[33] K.N. Boldirev, B.N. Mavrin, M.N. Popova, L.N. Bezmaternykh, Spectroscopy of phonon and vibronic states of $YbAl_3(BO_3)_4$ single crystal, Opt. Spectrosc. 111 (2011) 420–425.

[34] A.V. Malakhovskii, V.V. Sokolov, I.A. Gudim, Optical and magneto-optical spectra and electron structure of $ErAl_3(BO_3)_4$ single crystal, J. Alloys Compd. 698 (2017) 364–374.